Adaptive detection of Rician targets

Olivier Besson

Correspondence

Adaptive Detection of Rician Targets

Olivier Besson

We address the problem of detecting a signal of interest in Gaussian noise with an unknown covariance matrix, when the amplitude of the signal fluctuates along the observations and follows a Rice distribution. This is typical of a target that consists of one large dominant scatterer and a collection of small independent scatterers. We formulate it as a composite hypothesis testing problem, for which we derive the generalized likelihood ratio test, and show that it ensures a constant false alarm rate. Numerical simulations enable to assess its performance for Rician as well as Swerling I and III targets. It is shown that the new detector incurs no loss for Swerling targets but can offer a significant improvement for Rician targets, especially when the number of training samples is small.

I. PROBLEM STATEMENT

Searching for a specific signature among a set of data is an ubiquitous problem in many applications, including radar, communications, or hyperspectral imaging to name a few. Given a collection of K_p observations of size N, which can be gathered in an $N \times K_p$ matrix $\mathbf{X}$, the problem amounts to deciding whether $\mathbf{X} = \mathbf{N}_x$ or $\mathbf{X} = \mathbf{v}\mathbf{a}^H + \mathbf{N}_x$, where $\mathbf{N}_x$ stands for the disturbance matrix, $\mathbf{v}$ is the sought signature, and $\mathbf{a}$ denotes its amplitude along the K_p observations, with the superscript $.^H$ denoting the conjugate transpose (Hermitian) operator. In a typical radar scenario, N is the number of pulses sent by the radar within a scan (coherent processing interval), K_p is the number of scans, and $\mathbf{v}$ corresponds to the target signature. Alternatively, the columns of $\mathbf{X}$ can represent different range gates when a range-spread target is to be detected. Observe that the model $\mathbf{v}\mathbf{a}^H$ for the useful signal implies that the target amplitude, which is related to its radar cross section (RCS), varies only from column to column. In other words, pulse-to-pulse RCS fluctuations are not considered, only scan-to-scan or range-gate-to-range-gate fluctuations are supposed to exist. As for the disturbance $\mathbf{N}_x$, a classical assumption is that its columns are independent and identically distributed according to a complex multivariate Gaussian distribution with zero mean and covariance matrix $\mathbf{\Sigma}$. Since the latter is generally unknown, it is assumed that a set of secondary data $\mathbf{Y} \in \mathbb{C}^{N \times K_s}$ is available, whose distribution matches that of $\mathbf{N}_x$. Therefore, the problem can be formulated as the following composite hypothesis testing

DOI. No. 10.1109/TAES.2023.3234454

Refereeing of this contribution was handled by F. Gini.

Author's address: The author is with the ISAE-SUPAERO, Université de Toulouse, 31055 Toulouse, France, E-mail: (olivier.besson@isae-supaero.fr).

problem:

$$\mathcal{H}_0 : \mathbf{X} \overset{d}{=} \mathbb{CN}\left(\mathbf{0}, \mathbf{\Sigma}, \mathbf{I}_{K_p}\right); \mathbf{Y} \overset{d}{=} \mathbb{CN}\left(\mathbf{0}, \mathbf{\Sigma}, \mathbf{I}_{K_s}\right)$$
$$\mathcal{H}_1 : \mathbf{X} \overset{d}{=} \mathbb{CN}\left(\mathbf{v}\mathbf{a}^H, \mathbf{\Sigma}, \mathbf{I}_{K_p}\right); \mathbf{Y} \overset{d}{=} \mathbb{CN}\left(\mathbf{0}, \mathbf{\Sigma}, \mathbf{I}_{K_s}\right). \quad (1)$$

In the previous equation, $\mathbb{CN}(\mathbf{M}, \mathbf{A}, \mathbf{B})$ stands for the complex matrix variate distribution whose density is proportional to $|\mathbf{A}|^{-q}|\mathbf{B}|^{-p}\text{etr}\{-(\mathbf{Z}-\mathbf{M})^H\mathbf{A}^{-1}(\mathbf{Z}-\mathbf{M})\mathbf{B}^{-1}\}$, where $\mathbf{A}^{-1}$ denotes the inverse of a nonsingular matrix $\mathbf{A}$, etr{.} and |.| stand for the exponential of the trace of a matrix and its determinant, respectively, and $\mathbf{I}_K$ is the identity matrix of size K. At this stage, it remains to set statistical assumptions about $\mathbf{a}$. The pioneering work to solve (1) is due to Kelly [1], [2] who assumed that $\mathbf{a}$ was deterministic. This assumption has the merits that no hypothesis is made regarding the target amplitude, and moreover, it leads to tractable mathematical derivations and a closed-form expression for the generalized likelihood ratio test (GLRT), namely

$$\text{GLR}_{\text{Kelly}} \equiv \frac{\mathbf{v}^H\mathbf{S}_y^{-1}\mathbf{v}}{\mathbf{v}^H\mathbf{S}_{xy}^{-1}\mathbf{v}} \quad (2)$$

where $\mathbf{S}_y = \mathbf{Y}\mathbf{Y}^H$ and $\mathbf{S}_{xy} = \mathbf{S}_x + \mathbf{S}_y$ with $\mathbf{S}_x = \mathbf{X}\mathbf{X}^H$. Kelly's GLRT has been considered for decades now as the benchmark detector for (1). However, among the radar community, Swerling models [3], [4] are widely recognized. Briefly stated, there exist four models: Swerling I and III targets have scan to scan RCS fluctuations, while Swerling II and IV targets exhibit pulse to pulse RCS fluctuations. For all the targets, the squared target amplitude is modeled as a chi-square distributed random variable with two degrees of freedom (DoFs) for Swerling I and II targets, and four DoFs for Swerling III and IV targets. Therefore, the target amplitude of a Swerling I or II target has a Rayleigh distribution. Surprisingly enough, the adaptive detection of Swerling I targets using a statistical framework similar to that of Kelly has been addressed only recently in [5], where the GLRT assuming that $\mathbf{a} \overset{d}{=} \mathbb{CN}(\mathbf{0}, \sigma_a^2\mathbf{I}_{K_p})$ is derived. Extension to Swerling III targets has been considered in [6], where a high-signal-to-noise-ratio approximation of the GLRT is derived and is shown to coincide with the GLRT for Swerling I targets. Now, Swerling III targets are generally interpreted as targets with "one large dominant scatterer together with a collection of small independent scatterers" [7]. As noted in the latter reference, such a model rather results in a Rice distribution. Actually, as evidenced in [8] when the dominant part of a Rician target constitutes a large part of the total reflection, then Swerling III and Rician targets are relatively closed in terms of their distributions. This closeness had also been reported in [9]. Consequently, rather than using a Swerling III target model, a Rician target model makes sense. Observe that such a model has also been advocated in multiple-input multiple-output radar systems [10], [11], [12], [13], [14]. The Rician target model amounts to assuming that $\mathbf{a} \overset{d}{=} \mathbb{CN}(\bar{a}\mathbf{1}, \sigma_a^2\mathbf{I}_{K_p})$, where $\mathbf{1}$ is a vector whose components are all equal to 1. Therefore, we consider herein a new composite hypothesis testing problem defined as

$$\mathcal{H}_0 : \begin{cases} \mathbf{X} \overset{d}{=} \mathbb{CN}\left(\mathbf{0}, \mathbf{\Sigma}, \mathbf{I}_{K_p}\right) \\ \mathbf{Y} \overset{d}{=} \mathbb{CN}\left(\mathbf{0}, \mathbf{\Sigma}, \mathbf{I}_{K_s}\right) \end{cases}$$
$$\mathcal{H}_1 : \begin{cases} \mathbf{X} \overset{d}{=} \mathbb{CN}\left(\bar{a}^*\mathbf{v}\mathbf{1}^H, \mathbf{\Sigma} + \sigma_a^2\mathbf{v}\mathbf{v}^H, \mathbf{I}_{K_p}\right) \\ \mathbf{Y} \overset{d}{=} \mathbb{CN}\left(\mathbf{0}, \mathbf{\Sigma}, \mathbf{I}_{K_s}\right) \end{cases} \quad (3)$$

where the parameters $\bar{a}$, σ_a^2, and $\mathbf{\Sigma}$ are unknown. Similarly to Kelly, we propose a GLRT approach given by

$$\frac{\max\limits_{\bar{a},\sigma_a^2,\mathbf{\Sigma}} p_1(\mathbf{X}, \mathbf{Y})}{\max\limits_{\mathbf{\Sigma}} p_0(\mathbf{X}, \mathbf{Y})} \underset{\mathcal{H}_0}{\overset{\mathcal{H}_1}{\gtrless}} T \quad (4)$$

where $p_0(\mathbf{X}, \mathbf{Y})$ and $p_1(\mathbf{X}, \mathbf{Y})$ are the probability density functions (PDF) under $\mathcal{H}_0$ and $\mathcal{H}_1$, and T is the threshold to be set for a given probability of false alarm P_{fa}. The main result is given by (19), which provides the expression of the GLRT for Rician targets. In addition, we show that the left-hand side of (4) has a distribution that does not depend on $\mathbf{\Sigma}$ under $\mathcal{H}_0$ so that T can be set irrespective of $\mathbf{\Sigma}$. Section II is devoted to the derivation of the GLRT and analysis of its false alarm rate. Its performance is evaluated in Section III. Finally, Section IV concludes this article.

II. GLRT FOR RICIAN TARGETS

In this section, we first derive the GLRT as given in (4). We consider as well a two-step GLRT where the generalized likelihood ratio (GLR) based on $\mathbf{X}$ only is derived assuming $\mathbf{\Sigma}$ to be known, before the latter is replaced by the sample covariance matrix of the training samples $\mathbf{Y}$. Then, we discuss their false alarm rates.

A. Derivation of GLRT

With no loss of generality, we assume that $\mathbf{v}$ is unit norm, and we let $\mathbf{V}_\perp$ be a semiunitary matrix such that $\mathbf{V}_\perp^H\mathbf{v} = \mathbf{0}$. We define the orthogonal matrix $\mathbf{V} = \begin{bmatrix}\mathbf{v} & \mathbf{V}_\perp\end{bmatrix}$ such that $\mathbf{V}^H\mathbf{v} = \mathbf{e}_1 = \begin{bmatrix}1 & 0 & \dots & 0\end{bmatrix}^T$. It will be more convenient to work with the transformed data $\tilde{\mathbf{X}} = \mathbf{V}^H\mathbf{X}$, $\tilde{\mathbf{Y}} = \mathbf{V}^H\mathbf{Y}$ and covariance matrix $\tilde{\mathbf{\Sigma}} = \mathbf{V}^H\mathbf{\Sigma}\mathbf{V}$. The PDFs of $(\tilde{\mathbf{X}}, \tilde{\mathbf{Y}})$ under each hypothesis are then given by

$$\begin{aligned} p_0(\tilde{\mathbf{X}}, \tilde{\mathbf{Y}}) &= \pi^{-NK_t}|\tilde{\mathbf{\Sigma}}|^{-K_t}\text{etr}\left\{-\tilde{\mathbf{X}}^H\tilde{\mathbf{\Sigma}}^{-1}\tilde{\mathbf{X}} - \tilde{\mathbf{Y}}^H\tilde{\mathbf{\Sigma}}^{-1}\tilde{\mathbf{Y}}\right\} \\ p_1(\tilde{\mathbf{X}}, \tilde{\mathbf{Y}}) &= \pi^{-NK_t}|\tilde{\mathbf{\Sigma}} + \sigma_a^2\mathbf{e}_1\mathbf{e}_1^H|^{-K_p}|\tilde{\mathbf{\Sigma}}|^{-K_s} \\ &\quad \times \text{etr}\left\{-\tilde{\mathbf{Y}}^H\tilde{\mathbf{\Sigma}}^{-1}\tilde{\mathbf{Y}}\right\} \\ &\quad \times \text{etr}\left\{-(\tilde{\mathbf{X}} - \bar{a}^*\mathbf{e}_1\mathbf{1}^H)^H(\tilde{\mathbf{\Sigma}} + \sigma_a^2\mathbf{e}_1\mathbf{e}_1^H)^{-1}\right. \\ &\quad \left.\times(\tilde{\mathbf{X}} - \bar{a}^*\mathbf{e}_1\mathbf{1}^H)\right\} \end{aligned} \quad (5)$$

where $K_t = K_p + K_s$. The maximum of $p_0(\tilde{\mathbf{X}}, \tilde{\mathbf{Y}})$ is achieved at $K_t^{-1}(\tilde{\mathbf{X}}\tilde{\mathbf{X}}^H + \tilde{\mathbf{Y}}\tilde{\mathbf{Y}}^H)$ and is thus

$$\begin{aligned} \max_{\tilde{\mathbf{\Sigma}}} p_0(\tilde{\mathbf{X}}, \tilde{\mathbf{Y}}) &\propto |\tilde{\mathbf{X}}\tilde{\mathbf{X}}^H + \tilde{\mathbf{Y}}\tilde{\mathbf{Y}}^H|^{-K_t} \\ &= |\mathbf{V}^H\left(\mathbf{S}_x + \mathbf{S}_y\right)\mathbf{V}|^{-K_t} \end{aligned}$$

$$
\begin{aligned}
&= \left| \begin{pmatrix} \mathbf{v}^H \mathbf{S}_{xy} \mathbf{v} & \mathbf{v}^H \mathbf{S}_{xy} \mathbf{V}_\perp \\ \mathbf{V}_\perp^H \mathbf{S}_{xy} \mathbf{v} & \mathbf{V}_\perp^H \mathbf{S}_{xy} \mathbf{V}_\perp \end{pmatrix} \right|^{-K_t} \\
&= |\mathbf{V}_\perp^H \mathbf{S}_{xy} \mathbf{V}_\perp|^{-K_t} \\
&\quad \times [\mathbf{v}^H \mathbf{S}_{xy} \mathbf{v} - \mathbf{v}^H \mathbf{S}_{xy} \mathbf{V}_\perp (\mathbf{V}_\perp^H \mathbf{S}_{xy} \mathbf{V}_\perp)^{-1} \mathbf{V}_\perp^H \mathbf{S}_{xy} \mathbf{v}]^{-K_t} \\
&= |\mathbf{V}_\perp^H \mathbf{S}_{xy} \mathbf{V}_\perp|^{-K_t} [\mathbf{v}^H \mathbf{S}_{xy}^{1/2} \mathbf{P}^\perp_{\mathbf{S}_{xy}^{1/2} \mathbf{V}_\perp} \mathbf{S}_{xy}^{1/2} \mathbf{v}]^{-K_t} \\
&= |\mathbf{V}_\perp^H \mathbf{S}_{xy} \mathbf{V}_\perp|^{-K_t} [\mathbf{v}^H \mathbf{S}_{xy}^{1/2} \mathbf{P}_{\mathbf{S}_{xy}^{-1/2} \mathbf{v}} \mathbf{S}_{xy}^{1/2} \mathbf{v}]^{-K_t} \\
&= |\mathbf{V}_\perp^H \mathbf{S}_{xy} \mathbf{V}_\perp|^{-K_t} [\mathbf{v}^H \mathbf{S}_{xy}^{-1} \mathbf{v}]^{K_t} \qquad (6)
\end{aligned}
$$

where $\propto$ means proportional to, and for any vector $\mathbf{u}$, we let $\mathbf{P}_\mathbf{u} = (\mathbf{u}^H \mathbf{u})^{-1} \mathbf{u}\mathbf{u}^H$ be the projection on the subspace spanned by $\mathbf{u}$, and $\mathbf{P}_\mathbf{u}^\perp$ be the projection on its orthogonal complement. Let us now turn to the maximization problem under hypothesis $\mathcal{H}_1$. Temporarily defining $\tilde{\mathbf{\Omega}} = \tilde{\mathbf{\Sigma}} + \sigma_a^2 \mathbf{e}_1 \mathbf{e}_1^H$, we have that

$$
\begin{aligned}
t &= \mathrm{Tr}\{(\tilde{\mathbf{X}} - \bar{a}^* \mathbf{e}_1 \mathbf{1}^H)^H \tilde{\mathbf{\Omega}}^{-1} (\tilde{\mathbf{X}} - \bar{a}^* \mathbf{e}_1 \mathbf{1}^H)\} \\
&= \mathrm{Tr}\{\tilde{\mathbf{X}}^H \tilde{\mathbf{\Omega}}^{-1} \tilde{\mathbf{X}}\} - \bar{a}^* \mathbf{1}^H \tilde{\mathbf{X}}^H \tilde{\mathbf{\Omega}}^{-1} \mathbf{e}_1 \\
&\quad - \bar{a} \mathbf{e}_1^H \tilde{\mathbf{\Omega}}^{-1} \tilde{\mathbf{X}} \mathbf{1} + |\bar{a}|^2 (\mathbf{1}^H \mathbf{1})(\mathbf{e}_1^H \tilde{\mathbf{\Omega}}^{-1} \mathbf{e}_1) \\
&= (\mathbf{1}^H \mathbf{1})(\mathbf{e}_1^H \tilde{\mathbf{\Omega}}^{-1} \mathbf{e}_1) \left| \bar{a} - \frac{\mathbf{1}^H \tilde{\mathbf{X}}^H \tilde{\mathbf{\Omega}}^{-1} \mathbf{e}_1}{(\mathbf{1}^H \mathbf{1})(\mathbf{e}_1^H \tilde{\mathbf{\Omega}}^{-1} \mathbf{e}_1)} \right|^2 \\
&\quad + \mathrm{Tr}\{\tilde{\mathbf{X}}^H \tilde{\mathbf{\Omega}}^{-1} \tilde{\mathbf{X}}\} - \frac{|\mathbf{e}_1^H \tilde{\mathbf{\Omega}}^{-1} \tilde{\mathbf{X}} \mathbf{1}|^2}{(\mathbf{1}^H \mathbf{1})(\mathbf{e}_1^H \tilde{\mathbf{\Omega}}^{-1} \mathbf{e}_1)} \qquad (7)
\end{aligned}
$$

from which we obtain

$$
\begin{aligned}
&\max_{\bar{a}} p_1(\tilde{\mathbf{X}}, \tilde{\mathbf{Y}}) \\
&= \pi^{-NK_t} |\tilde{\mathbf{\Omega}}|^{-K_p} |\tilde{\mathbf{\Sigma}}|^{-K_s} \mathrm{etr}\left\{ -\tilde{\mathbf{Y}}^H \tilde{\mathbf{\Sigma}}^{-1} \tilde{\mathbf{Y}} \right\} \\
&\quad \times \mathrm{etr}\left\{ -\tilde{\mathbf{X}}^H \tilde{\mathbf{\Omega}}^{-1} \tilde{\mathbf{X}} \right\} \exp\left\{ \frac{|\mathbf{e}_1^H \tilde{\mathbf{\Omega}}^{-1} \tilde{\mathbf{X}} \mathbf{1}|^2}{(\mathbf{1}^H \mathbf{1})(\mathbf{e}_1^H \tilde{\mathbf{\Omega}}^{-1} \mathbf{e}_1)} \right\}. \qquad (8)
\end{aligned}
$$

Let us partition $\tilde{\mathbf{\Sigma}}$ and $\tilde{\mathbf{\Omega}}$ as

$$
\tilde{\mathbf{\Sigma}} = \begin{pmatrix} \tilde{\Sigma}_{11} & \tilde{\mathbf{\Sigma}}_{12} \\ \tilde{\mathbf{\Sigma}}_{21} & \tilde{\mathbf{\Sigma}}_{22} \end{pmatrix}, \; \tilde{\mathbf{\Omega}} = \begin{pmatrix} \tilde{\Sigma}_{11} + \sigma_a^2 & \tilde{\mathbf{\Sigma}}_{12} \\ \tilde{\mathbf{\Sigma}}_{21} & \tilde{\mathbf{\Sigma}}_{22} \end{pmatrix}. \qquad (9)
$$

We can write that

$$
\tilde{\mathbf{\Sigma}}^{-1} = \tilde{\Sigma}_{1.2}^{-1} \begin{bmatrix} 1 \\ -\tilde{\mathbf{t}}_{21} \end{bmatrix} \begin{bmatrix} 1 & -\tilde{\mathbf{t}}_{21}^H \end{bmatrix} + \begin{pmatrix} 0 & \mathbf{0} \\ \mathbf{0} & \tilde{\mathbf{\Sigma}}_{22}^{-1} \end{pmatrix} \qquad (10)
$$

with $\tilde{\mathbf{t}}_{21} = \tilde{\mathbf{\Sigma}}_{22}^{-1} \tilde{\mathbf{\Sigma}}_{21}$ and $\tilde{\Sigma}_{1.2} = \tilde{\Sigma}_{11} - \tilde{\mathbf{\Sigma}}_{12} \tilde{\mathbf{\Sigma}}_{22}^{-1} \tilde{\mathbf{\Sigma}}_{21}$. A similar equation is obtained with $\tilde{\mathbf{\Omega}}^{-1}$ with the difference $\tilde{\Omega}_{1.2} = \tilde{\Sigma}_{1.2} + \sigma_a^2$. We reparameterize the unknown $\tilde{\mathbf{\Sigma}}$ in terms of the new and equivalent unknowns $\tilde{\Sigma}_{1.2}$, $\tilde{\mathbf{t}}_{21}$ and $\tilde{\mathbf{\Sigma}}_{22}$. Doing so, we obtain

$$
\begin{aligned}
\mathbf{e}_1^H \tilde{\mathbf{\Omega}}^{-1} \mathbf{e}_1 &= (\tilde{\Sigma}_{1.2} + \sigma_a^2)^{-1} \\
\mathbf{e}_1^H \tilde{\mathbf{\Omega}}^{-1} \tilde{\mathbf{X}} \mathbf{1} &= (\tilde{\Sigma}_{1.2} + \sigma_a^2)^{-1} \begin{bmatrix} 1 & -\tilde{\mathbf{t}}_{21}^H \end{bmatrix} \tilde{\mathbf{X}} \mathbf{1} \\
\mathrm{Tr}\{\tilde{\mathbf{X}}^H \tilde{\mathbf{\Omega}}^{-1} \tilde{\mathbf{X}}\} &= (\tilde{\Sigma}_{1.2} + \sigma_a^2)^{-1} \begin{bmatrix} 1 & -\tilde{\mathbf{t}}_{21}^H \end{bmatrix} \tilde{\mathbf{X}} \tilde{\mathbf{X}}^H \begin{bmatrix} 1 \\ -\tilde{\mathbf{t}}_{21} \end{bmatrix} \\
&\quad + \mathrm{Tr}\{\tilde{\mathbf{X}}_2^H \tilde{\mathbf{\Sigma}}_{22}^{-1} \tilde{\mathbf{X}}_{22}\} \qquad (11)
\end{aligned}
$$

where we have partitioned $\tilde{\mathbf{X}}$ as $\tilde{\mathbf{X}} = \begin{bmatrix} \tilde{\mathbf{X}}_1 \\ \tilde{\mathbf{X}}_2 \end{bmatrix}$. Next, for any matrix $\tilde{\mathbf{\Gamma}}$ partitioned as in (9), we have

$$
\begin{aligned}
&\begin{bmatrix} 1 & -\tilde{\mathbf{t}}_{21}^H \end{bmatrix} \tilde{\mathbf{\Gamma}} \begin{bmatrix} 1 \\ -\tilde{\mathbf{t}}_{21} \end{bmatrix} = \tilde{\Gamma}_{1.2} \\
&\quad + (\tilde{\mathbf{t}}_{21} - \tilde{\mathbf{\Gamma}}_{22}^{-1} \tilde{\mathbf{\Gamma}}_{21})^H \tilde{\mathbf{\Gamma}}_{22} (\tilde{\mathbf{t}}_{21} - \tilde{\mathbf{\Gamma}}_{22}^{-1} \tilde{\mathbf{\Gamma}}_{21}) \qquad (12)
\end{aligned}
$$

with $\tilde{\Gamma}_{1.2} = \tilde{\Gamma}_{11} - \tilde{\mathbf{\Gamma}}_{12} \tilde{\mathbf{\Gamma}}_{22}^{-1} \tilde{\mathbf{\Gamma}}_{21}$. Finally, using $|\tilde{\mathbf{\Sigma}}| = \tilde{\Sigma}_{1.2} \, |\tilde{\mathbf{\Sigma}}_{22}|$, one gets

$$
\begin{aligned}
\max_{\bar{a}} p_1(\tilde{\mathbf{X}}, \tilde{\mathbf{Y}}) &\propto (\tilde{\Sigma}_{1.2} + \sigma_a^2)^{-K_p} \tilde{\Sigma}_{1.2}^{-K_s} \exp\{-\tilde{\Gamma}_{1.2}\} \\
&\quad \times |\tilde{\mathbf{\Sigma}}_{22}|^{-K_t} \mathrm{etr}\left\{ -\tilde{\mathbf{X}}_2^H \tilde{\mathbf{\Sigma}}_{22}^{-1} \tilde{\mathbf{X}}_2 - \tilde{\mathbf{Y}}_2^H \tilde{\mathbf{\Sigma}}_{22}^{-1} \tilde{\mathbf{Y}}_2 \right\} \\
&\quad \times \exp\{-(\tilde{\mathbf{t}}_{21} - \tilde{\mathbf{\Gamma}}_{22}^{-1} \tilde{\mathbf{\Gamma}}_{21})^H \tilde{\mathbf{\Gamma}}_{22} (\tilde{\mathbf{t}}_{21} - \tilde{\mathbf{\Gamma}}_{22}^{-1} \tilde{\mathbf{\Gamma}}_{21})\} \qquad (13)
\end{aligned}
$$

where

$$
\begin{aligned}
\tilde{\mathbf{\Gamma}} &= \tilde{\Sigma}_{1.2}^{-1} \tilde{\mathbf{Y}} \tilde{\mathbf{Y}}^H + (\tilde{\Sigma}_{1.2} + \sigma_a^2)^{-1} \left[\tilde{\mathbf{X}} \tilde{\mathbf{X}}^H - \tilde{\mathbf{X}} \frac{\mathbf{1}\mathbf{1}^H}{\mathbf{1}^H \mathbf{1}} \tilde{\mathbf{X}}^H \right] \\
&= \tilde{\Sigma}_{1.2}^{-1} \tilde{\mathbf{Y}} \tilde{\mathbf{Y}}^H + (\tilde{\Sigma}_{1.2} + \sigma_a^2)^{-1} \tilde{\mathbf{X}} \mathbf{P}_\mathbf{1}^\perp \tilde{\mathbf{X}}^H \\
&= \mathbf{V}^H \left[\tilde{\Sigma}_{1.2}^{-1} \mathbf{S}_y + (\tilde{\Sigma}_{1.2} + \sigma_a^2)^{-1} \mathbf{X} \mathbf{P}_\mathbf{1}^\perp \mathbf{X}^H \right] \mathbf{V}. \qquad (14)
\end{aligned}
$$

The maximum likelihood estimates (MLEs) of $\tilde{\mathbf{\Sigma}}_{22}$ and $\tilde{\mathbf{t}}_{21}$ are, thus, $K_t^{-1}(\tilde{\mathbf{X}}_2 \tilde{\mathbf{X}}_2^H + \tilde{\mathbf{Y}}_2 \tilde{\mathbf{Y}}_2^H)$ and $\tilde{\mathbf{\Gamma}}_{22}^{-1} \tilde{\mathbf{\Gamma}}_{21}$, respectively, and we end up with

$$
\begin{aligned}
\max_{\bar{a}, \tilde{\mathbf{\Sigma}}_{22}, \tilde{\mathbf{t}}_{21}} p_1(\tilde{\mathbf{X}}, \tilde{\mathbf{Y}}) &\propto |\mathbf{V}_\perp^H (\mathbf{S}_x + \mathbf{S}_y) \mathbf{V}_\perp|^{-K_t} \\
&\quad \times (\tilde{\Sigma}_{1.2} + \sigma_a^2)^{-K_p} \tilde{\Sigma}_{1.2}^{-K_s} \exp\{-\tilde{\Gamma}_{1.2}\} \qquad (15)
\end{aligned}
$$

where we used the fact that $\tilde{\mathbf{X}}_2 = \mathbf{V}_\perp^H \mathbf{X}$. The only unknowns that remain are now $\tilde{\Sigma}_{1.2}$ and σ_a^2. Let us rewrite $\tilde{\Gamma}_{1.2}$ explicitly in terms of these variables. $\tilde{\Gamma}_{1.2}^{-1}$ is the (1,1) element of $\tilde{\mathbf{\Gamma}}^{-1}$, and from (14), one has

$$
\tilde{\Gamma}_{1.2}^{-1} = \mathbf{v}^H \left[\tilde{\Sigma}_{1.2}^{-1} \mathbf{S}_y + (\tilde{\Sigma}_{1.2} + \sigma_a^2)^{-1} \mathbf{X} \mathbf{P}_\mathbf{1}^\perp \mathbf{X}^H \right]^{-1} \mathbf{v}. \qquad (16)
$$

At this stage, it is relevant to note that if $K_p = 1$, $\mathbf{X}$ boils down to a vector and $\mathbf{X} \mathbf{P}_\mathbf{1}^\perp \mathbf{X}^H = \mathbf{0}$, which means that $\tilde{\Gamma}_{1.2}^{-1}$ does not depend on σ_a^2 and (15) will depend on σ_a^2 only through $(\tilde{\Sigma}_{1.2} + \sigma_a^2)^{-1}$. Therefore, the GLR becomes unbounded, which shows that the model is not identifiable. This makes sense since there are two unknowns ($\bar{a}$ and σ_a^2) for a single vector in the primary data. Hence, in the following, we assume that $K_p > 1$. Making the change of variables $(\tilde{\Sigma}_{1.2}, \sigma_a^2) \to (\alpha = \tilde{\Sigma}_{1.2}, \beta = \tilde{\Sigma}_{1.2}(\tilde{\Sigma}_{1.2} + \sigma_a^2)^{-1})$, we need to maximize

$$
f(\alpha, \beta) = \alpha^{-K_t} \beta^{K_p} \exp\{-\alpha^{-1} [\mathbf{v}^H (\mathbf{S}_y + \beta \mathbf{X} \mathbf{P}_\mathbf{1}^\perp \mathbf{X}^H)^{-1} \mathbf{v}]^{-1}\}. \qquad (17)
$$

It is straightforward to see that, for a fixed β, the maximum over α is achieved at $K_t^{-1} [\mathbf{v}^H (\mathbf{S}_y + \beta \mathbf{X} \mathbf{P}_\mathbf{1}^\perp \mathbf{X}^H)^{-1} \mathbf{v}]^{-1}$, from which we get

$$
\begin{aligned}
\max_{\bar{a}, \tilde{\mathbf{\Sigma}}_{22}, \tilde{\mathbf{t}}_{21}, \alpha} p_1(\tilde{\mathbf{X}}, \tilde{\mathbf{Y}}) &\propto |\mathbf{V}_\perp^H (\mathbf{S}_x + \mathbf{S}_y) \mathbf{V}_\perp|^{-K_t} \\
&\quad \times \beta^{K_p} [\mathbf{v}^H (\mathbf{S}_y + \beta \mathbf{X} \mathbf{P}_\mathbf{1}^\perp \mathbf{X}^H)^{-1} \mathbf{v}]^{K_t}. \qquad (18)
\end{aligned}
$$

Using the previous equation along with (6), the GLR is finally given by

$$\mathrm{GLR}_{\mathrm{Rice}} \equiv \frac{\max\limits_{0<\beta<1} \beta^{K_p/K_t}[\mathbf{v}^H(\mathbf{S}_y + \beta\mathbf{X}\mathbf{P}_\mathbf{1}^\perp\mathbf{X}^H)^{-1}\mathbf{v}]}{\mathbf{v}^H(\mathbf{S}_y + \mathbf{X}\mathbf{X}^H)^{-1}\mathbf{v}}. \quad (19)$$

An important observation here is that the GLR can be computed provided that $\mathbf{S}_y + \beta\mathbf{X}\mathbf{P}_\mathbf{1}^\perp\mathbf{X}^H$ is nonsingular. However, the rank of this matrix is $K_s + K_p - 1$, and hence, *we only need that* $K_p + K_s > N$, not necessarily $K_s \geq N$, the latter condition being required for implementing Kelly's GLRT.

A few words are in order concerning solving the maximization problem in (19). Since we need to maximize a continuous and bounded scalar function over the finite interval]0,1[, the easiest way is to evaluate the function over a grid of values. More precisely, we first find the maximum over a coarse grid and then refine estimation of β on a finer grid. The complexity mostly lies in evaluating $f(\beta) = \mathbf{v}^H(\mathbf{S}_y + \beta\mathbf{X}\mathbf{P}_\mathbf{1}^\perp\mathbf{X}^H)^{-1}\mathbf{v}$. Toward this end, let $\mathbf{F}$ be a semiunitary matrix whose columns are all orthogonal to $\mathbf{1}$ so that $\mathbf{P}_\mathbf{1}^\perp = \mathbf{F}\mathbf{F}^H$ and let

$$\begin{bmatrix}\mathbf{F}^H\mathbf{X}^H \\ \mathbf{Y}^H\end{bmatrix} = \mathbf{Q}\mathbf{R} = \begin{bmatrix}\mathbf{Q}_x \\ \mathbf{Q}_y\end{bmatrix}\mathbf{R} \quad (20)$$

be a thin QR decomposition. In addition, let $\mathbf{Q}_x^H = \mathbf{U}_x\mathbf{\Sigma}_x\mathbf{V}_x^H$ denote the thin SVD of $\mathbf{Q}_x^H$, where $\mathbf{U}_x$ has $R = \min(N, K_p - 1)$ columns and $\mathbf{\Sigma}_x = \mathrm{diag}(\sigma_1, \ldots, \sigma_R)$. Then, $f(\beta)$ can be readily evaluated as

$$f(\beta) = \left\|\mathbf{R}^{-H}\mathbf{v}\right\|^2 + (1-\beta)\sum_{r=1}^{R}\frac{\sigma_r^2|[\mathbf{U}_x^H\mathbf{R}^{-H}\mathbf{v}]_r|^2}{1+(\beta-1)\sigma_r^2}. \quad (21)$$

B. Two-Step GLRT

Another possible approach that has been popularized by Robey et al. [15] and is referred to as the adaptive matched filter is to resort to a two-step GLRT. More precisely, the GLR is first derived based on $\mathbf{X}$ only assuming that $\mathbf{\Sigma}$ is known. Then, the latter is replaced by the sample covariance matrix of $\mathbf{Y}$, namely $K_s^{-1}\mathbf{S}_y$. Let us thus assume first that $\mathbf{\Sigma}$ is known. Then

$$\begin{aligned} p_0(\tilde{\mathbf{X}}) &= \pi^{-NK_p}|\tilde{\mathbf{\Sigma}}|^{-K_p}\mathrm{etr}\left\{-\tilde{\mathbf{X}}^H\tilde{\mathbf{\Sigma}}^{-1}\tilde{\mathbf{X}}\right\} \\ p_1(\tilde{\mathbf{X}}) &= \pi^{-NK_p}|\tilde{\mathbf{\Omega}}|^{-K_p} \\ &\quad\times \mathrm{etr}\left\{-(\tilde{\mathbf{X}} - \bar{a}^*\mathbf{e}_1\mathbf{1}^H)^H\tilde{\mathbf{\Omega}}^{-1}(\tilde{\mathbf{X}} - \bar{a}^*\mathbf{e}_1\mathbf{1}^H)\right\}. \end{aligned} \quad (22)$$

From (8), we have

$$\begin{aligned} \max_{\bar{a}} p_1(\tilde{\mathbf{X}}) &= \pi^{-NK_p}|\tilde{\mathbf{\Omega}}|^{-K_p}\mathrm{etr}\left\{-\tilde{\mathbf{X}}^H\tilde{\mathbf{\Omega}}^{-1}\tilde{\mathbf{X}}\right\} \\ &\quad\times \exp\left\{\frac{|\mathbf{e}_1^H\tilde{\mathbf{\Omega}}^{-1}\tilde{\mathbf{X}}\mathbf{1}|^2}{(\mathbf{1}^H\mathbf{1})(\mathbf{e}_1^H\tilde{\mathbf{\Omega}}^{-1}\mathbf{e}_1)}\right\} \end{aligned} \quad (23)$$

which can be readily rewritten as

$$\begin{aligned} \max_{\bar{a}} p_1(\tilde{\mathbf{X}}) &= p_0(\tilde{\mathbf{X}})\tilde{\Sigma}_{1.2}^{K_p}(\tilde{\Sigma}_{1.2} + \sigma_a^2)^{-K_p} \\ &\quad\times \exp\left\{\frac{\sigma_a^2\tilde{\Sigma}_{1.2}\mathbf{e}_1^H\tilde{\mathbf{\Sigma}}^{-1}\tilde{\mathbf{X}}\tilde{\mathbf{X}}^H\tilde{\mathbf{\Sigma}}^{-1}\mathbf{e}_1}{\tilde{\Sigma}_{1.2} + \sigma_a^2}\right\} \\ &\quad\times \exp\left\{\frac{\tilde{\Sigma}_{1.2}^2\mathbf{e}_1^H\tilde{\mathbf{\Sigma}}^{-1}\tilde{\mathbf{X}}\mathbf{P}_\mathbf{1}\tilde{\mathbf{X}}^H\tilde{\mathbf{\Sigma}}^{-1}\mathbf{e}_1}{\tilde{\Sigma}_{1.2} + \sigma_a^2}\right\}. \end{aligned} \quad (24)$$

It follows that the GLR for given $\mathbf{\Sigma}$ is given by

$$\mathrm{GLR}|\mathbf{\Sigma} \equiv \max_{\sigma_a^2} a^{K_p}(a+\sigma_a^2)^{-K_p}\exp\left\{\frac{b\sigma_a^2 + c}{a+\sigma_a^2}\right\} \quad (25)$$

where

$$\begin{aligned} a &= \tilde{\Sigma}_{1.2} = (\mathbf{v}^H\mathbf{\Sigma}^{-1}\mathbf{v})^{-1} \\ b &= \tilde{\Sigma}_{1.2}\mathbf{e}_1^H\tilde{\mathbf{\Sigma}}^{-1}\tilde{\mathbf{X}}\tilde{\mathbf{X}}^H\tilde{\mathbf{\Sigma}}^{-1}\mathbf{e}_1 \\ &= (\mathbf{v}^H\mathbf{\Sigma}^{-1}\mathbf{v})^{-1}(\mathbf{v}^H\mathbf{\Sigma}^{-1}\mathbf{S}_x\mathbf{\Sigma}^{-1}\mathbf{v}) \\ c &= \tilde{\Sigma}_{1.2}^2\mathbf{e}_1^H\tilde{\mathbf{\Sigma}}^{-1}\tilde{\mathbf{X}}\mathbf{P}_\mathbf{1}\tilde{\mathbf{X}}^H\tilde{\mathbf{\Sigma}}^{-1}\mathbf{e}_1 \\ &= (\mathbf{v}^H\mathbf{\Sigma}^{-1}\mathbf{v})^{-2}(\mathbf{v}^H\mathbf{\Sigma}^{-1}\mathbf{X}\mathbf{P}_\mathbf{1}\mathbf{X}^H\mathbf{\Sigma}^{-1}\mathbf{v}). \end{aligned} \quad (26)$$

The problem in (25) can be solved rather easily (we omit the details) yielding

$$\mathrm{GLR}|\mathbf{\Sigma} \equiv h\left(\max(b - c/a, K_p)\right) \quad (27)$$

with

$$h(x) = (x/K_p)^{-K_p}\exp\{x + c/a - K_p\}. \quad (28)$$

It remains to replace $\mathbf{\Sigma}$ by $K_s^{-1}\mathbf{S}_y$ in (26) and (27) to obtain the two-step GLR. Note that such a two-step GLRT requires that $\mathbf{S}_y$ is nonsingular, which requires that $K_s \geq N$, a more severe constraint than that of the (one-step) GLRT. Actually, in the simulations, we are mostly interested in a scenario where K_s is of the order of N, a situation where the one-step GLRT typically performs better than the two-step GLRT. The two detectors will be compared in the next section through numerical simulations.

C. Constant False Alarm Rate

We show below that the GLRT enjoys the so-called constant false alarm rate (CFAR). Toward this end, let us note that the GLR is obtained by maximizing $\beta^{K_p/K_t}g(\beta, \mathbf{X}, \mathbf{Y})$, where

$$g(\beta, \mathbf{X}, \mathbf{Y}) = \frac{\mathbf{v}^H(\mathbf{Y}\mathbf{Y}^H + \beta\mathbf{X}\mathbf{P}_\mathbf{1}^\perp\mathbf{X}^H)^{-1}\mathbf{v}}{\mathbf{v}^H(\mathbf{Y}\mathbf{Y}^H + \mathbf{X}\mathbf{X}^H)^{-1}\mathbf{v}}. \quad (29)$$

Now, one can write $\mathbf{X} = \mathbf{\Sigma}^{\frac{1}{2}}(\mathbf{N}_x + \bar{a}^*\mathbf{\Sigma}^{-\frac{1}{2}}\mathbf{v}\mathbf{1}^H)$ and $\mathbf{Y} = \mathbf{\Sigma}^{\frac{1}{2}}\mathbf{N}_y$, where $\mathbf{N}_x \overset{d}{=} \mathbb{C}\mathcal{N}(\mathbf{0}, \mathbf{I}_N, \mathbf{I}_{K_p})$ and $\mathbf{N}_y \overset{d}{=} \mathbb{C}\mathcal{N}(\mathbf{0}, \mathbf{I}_N, \mathbf{I}_{K_s})$. Note also that $\mathbf{N}_x \overset{d}{=} \mathbf{Q}^H\mathbf{N}_x$ and $\mathbf{N}_y \overset{d}{=} \mathbf{Q}^H\mathbf{N}_y$ for any unitary matrix $\mathbf{Q}$. Therefore, under $\mathcal{H}_0$

$$\begin{aligned} g(\beta, \mathbf{X}, \mathbf{Y}) &= \frac{\mathbf{v}^H(\mathbf{Y}\mathbf{Y}^H + \beta\mathbf{X}\mathbf{P}_\mathbf{1}^\perp\mathbf{X}^H)^{-1}\mathbf{v}}{\mathbf{v}^H(\mathbf{Y}\mathbf{Y}^H + \mathbf{X}\mathbf{X}^H)^{-1}\mathbf{v}} \\ &= \frac{\mathbf{v}^H\mathbf{\Sigma}^{-\frac{1}{2}}(\mathbf{N}_y\mathbf{N}_y^H + \beta\mathbf{N}_x\mathbf{P}_\mathbf{1}^\perp\mathbf{N}_x^H)^{-1}\mathbf{\Sigma}^{-\frac{1}{2}}\mathbf{v}}{\mathbf{v}^H\mathbf{\Sigma}^{-\frac{1}{2}}(\mathbf{N}_y\mathbf{N}_y^H + \mathbf{N}_x\mathbf{N}_x^H)^{-1}\mathbf{\Sigma}^{-\frac{1}{2}}\mathbf{v}} \\ &\overset{d}{=} \frac{\mathbf{v}^H\mathbf{\Sigma}^{-\frac{1}{2}}\mathbf{Q}(\mathbf{N}_y\mathbf{N}_y^H + \beta\mathbf{N}_x\mathbf{P}_\mathbf{1}^\perp\mathbf{N}_x^H)^{-1}\mathbf{Q}^H\mathbf{\Sigma}^{-\frac{1}{2}}\mathbf{v}}{\mathbf{v}^H\mathbf{\Sigma}^{-\frac{1}{2}}\mathbf{Q}(\mathbf{N}_y\mathbf{N}_y^H + \mathbf{N}_x\mathbf{N}_x^H)^{-1}\mathbf{Q}^H\mathbf{\Sigma}^{-\frac{1}{2}}\mathbf{v}} \end{aligned}$$

$$= \frac{\mathbf{e}_1^H(\mathbf{N}_y\mathbf{N}_y^H + \beta\mathbf{N}_x\mathbf{P}_{\mathbf{1}}^{\perp}\mathbf{N}_x^H)^{-1}\mathbf{e}_1}{\mathbf{e}_1^H(\mathbf{N}_y\mathbf{N}_y^H + \mathbf{N}_x\mathbf{N}_x^H)^{-1}\mathbf{e}_1} \tag{30}$$

where, to obtain the last line, we have chosen $\mathbf{Q}$ such that $\mathbf{Q}^H\boldsymbol{\Sigma}^{-\frac{1}{2}}\mathbf{v} = (\mathbf{v}^H\boldsymbol{\Sigma}^{-1}\mathbf{v})^{1/2}\mathbf{e}_1$. Consequently, the distribution of $g(\beta, \mathbf{X}, \mathbf{Y})$ is independent of $\boldsymbol{\Sigma}$, and hence, the GLRT is CFAR.

Similarly, it is readily seen that $b - c/a$ has a distribution that is independent of $\boldsymbol{\Sigma}$ under $\mathcal{H}_0$, which means that the two-step GLRT is also CFAR.

III. PERFORMANCE EVALUATION

The aim of this section is to evaluate the performance of the new schemes both for estimation and detection purposes. We consider scenario with $N = 16$. The target signature is given by $\mathbf{v} = N^{-1/2}\left[1 \quad e^{i2\pi f_t} \quad \dots \quad e^{i2\pi(N-1)f_t}\right]^T$ with $f_t = 0.09$. The covariance matrix is $\boldsymbol{\Sigma} = \boldsymbol{\Sigma}_c + \sigma_n^2\mathbf{I}_N$, where $[\boldsymbol{\Sigma}_c]_{m_1,m_2} = \exp\{-2\pi^2\sigma_f^2(m_1 - m_2)^2\}$ with $\sigma_f = 0.01$ and σ_n^2 is set such that $\mathrm{Tr}\{\boldsymbol{\Sigma}_c\}/\mathrm{Tr}\{\sigma_n^2\mathbf{I}_N\} = 20$ dB. The signal-to-noise ratio is defined as $\mathrm{SNR} = P\mathbf{v}^H\boldsymbol{\Sigma}^{-1}\mathbf{v}$. When dealing with Rician targets, we have $P = |\bar{a}|^2 + \sigma_a^2 = \varepsilon P + (1 - \varepsilon)P$, where $\varepsilon = |\bar{a}|^2/(|\bar{a}|^2 + \sigma_a^2)$ represents the fraction of the dominant scatterer to the total reflection. The amplitude $\mathbf{a}$ is generated as $\mathbf{a} \overset{d}{=} \mathbb{CN}(\bar{a}\mathbf{1}, \sigma_a^2\mathbf{I}_{K_p})$ with $\bar{a} = |\bar{a}|e^{i\psi}$ and ψ is uniformly distributed over $[0, 2\pi[$. We will also consider Swerling I and Swerling III targets. For the former, we generate $\mathbf{a}$ from $\mathbf{a} \overset{d}{=} \mathbb{CN}(\mathbf{0}, P\mathbf{I}_{K_p})$. As for Swerling III targets, the elements of $\mathbf{a}$ are independent and identically distributed as $\mathbf{a}_k = \frac{\sqrt{P}}{2}|\mathbf{a}_k|e^{i\phi_k}$ with $|\mathbf{a}_k| \overset{d}{=} \sqrt{\chi_4^2(0)}$ and ϕ_k is uniformly distributed over $[0, 2\pi[$.

A. Estimation

The derivations above, although primarily devoted to obtaining the GLR, also provide MLEs of $\bar{a}$ and σ_a^2 under $\mathcal{H}_1$. Therefore, we first focus on the estimation of these two parameters. We assume a Rician target, and we display in Figs. 1 and 2 the average value (over 300 Monte Carlo trials) of $|\hat{\bar{a}}|^2$, $\hat{\sigma}_a^2$, and $\hat{P} = |\hat{\bar{a}}|^2 + \hat{\sigma}_a^2$ versus SNR for different values of ε. One can observe that the algorithm provides rather accurate estimates of P, especially for $K_s = 2N$, and that it enables to distinguish the respective contributions of $|\bar{a}|^2$ (dominant scatterer) and σ_a^2 (small independent scatterers). Moreover, with Swerling I targets ($\varepsilon = 0$), the MLE results in small values of $|\hat{\bar{a}}|^2$ and $\hat{P} \simeq \hat{\sigma}_a^2$, which is meaningful.

Next, a Swerling III target is considered. In this case, the parameters $\bar{a}$ and σ_a^2 are irrelevant. However, one can compare the estimated value of $|\bar{a}|^2 + \sigma_a^2$ to P, and also, see how the power is balanced between the two terms. This is reported in Fig. 3, where different values of K_p and K_s are used. The first thing to be noted is that the estimates of P can be rather accurate (especially at $K_s = 32$) and that the algorithm mostly recognizes that $|\bar{a}|$ is small and subsequently approximates P by σ_a^2. In other words, the algorithm fits a Rician model with small $|\bar{a}|$ and $\sigma_a^2 \simeq P$ on

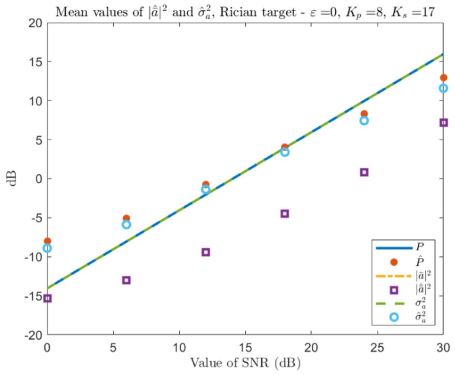

(a)

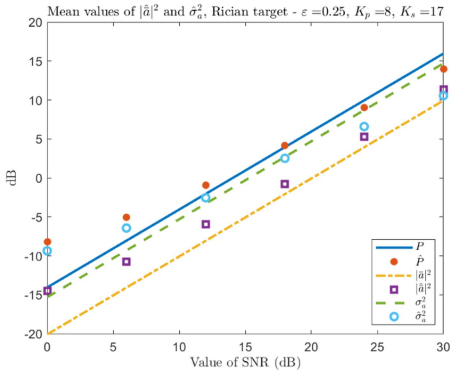

(b)

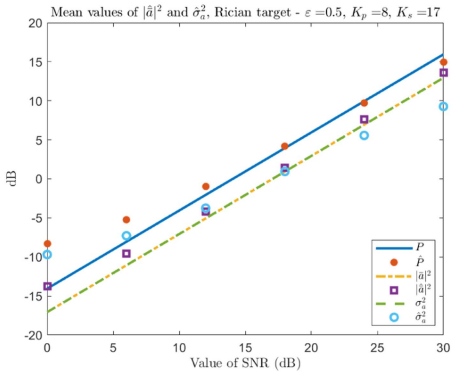

(c)

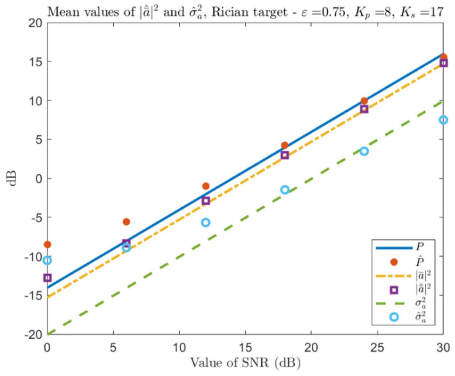

(d)

Fig. 1. Rician target: mean values of $|\hat{\bar{a}}|^2$, $\hat{\sigma}_a^2$ and $\hat{P} = |\hat{\bar{a}}|^2 + \hat{\sigma}_a^2$ versus SNR for various ε. $K_p = 8$ and $K_s = 17$. (a) $\varepsilon = 0$ (Swerling I). (b) $\varepsilon = 0.25$. (c) $\varepsilon = 0.5$. (d) $\varepsilon = 0.75$.

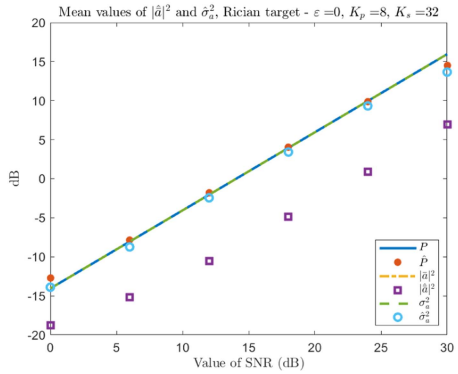

(a)

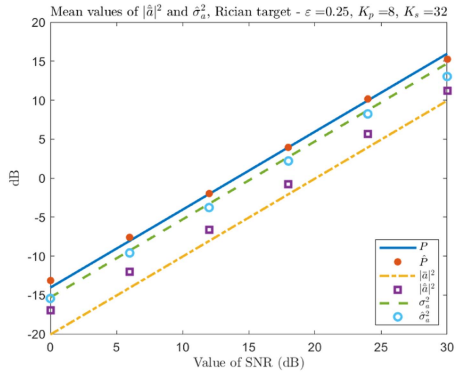

(b)

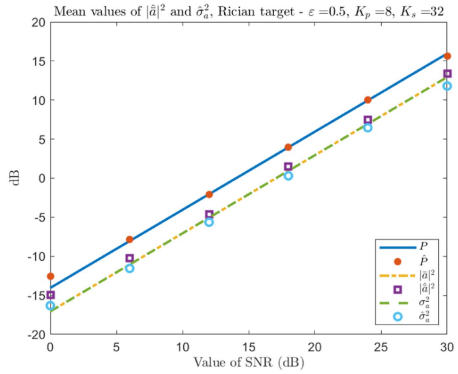

(c)

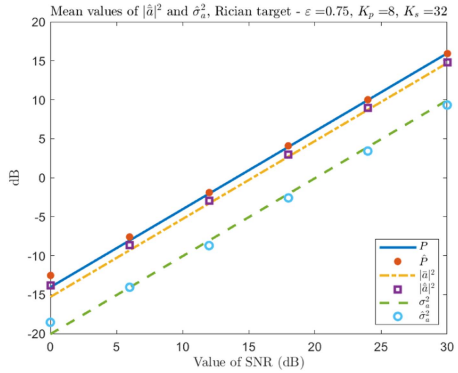

(d)

Fig. 2. Rician target: mean values of $|\hat{\tilde{a}}|^2$, $\hat{\sigma}_a^2$, and $\hat{P} = |\hat{\tilde{a}}|^2 + \hat{\sigma}_a^2$ versus SNR for various ε. $K_p = 8$ and $K_s = 32$. (a) $\varepsilon = 0$ (Swerling I). (b) $\varepsilon = 0.25$. (c) $\varepsilon = 0.5$. (d) $\varepsilon = 0.75$.

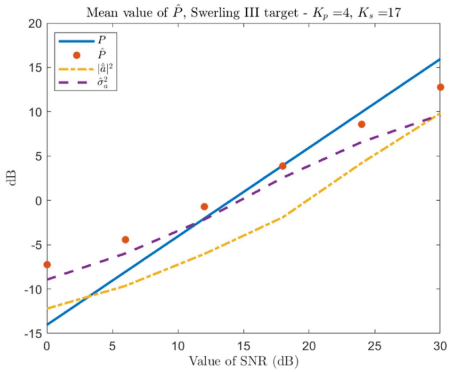

(a)

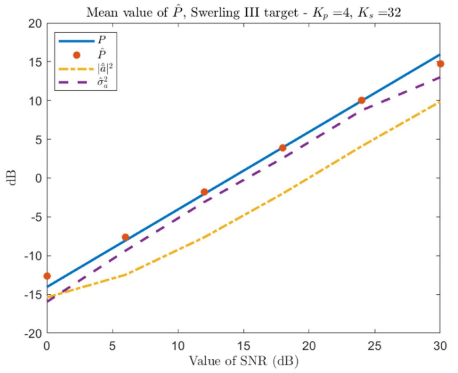

(b)

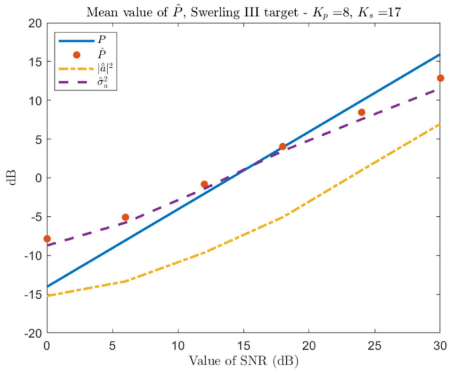

(c)

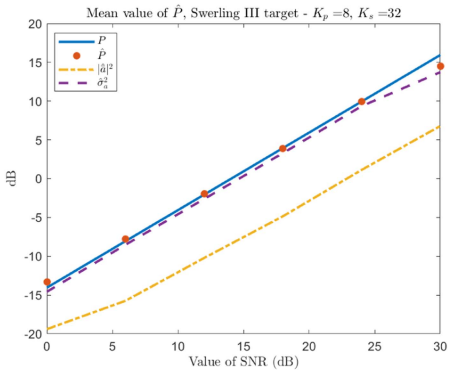

(d)

Fig. 3. Swerling III target: mean value of $\hat{P}$ versus SNR for various K_p and K_s. (a) $K_p = N/4$, $K_s = N + 1$. (b) $K_p = N/4$, $K_s = 2N$. (c) $K_p = N/2$, $K_s = N + 1$. (d) $K_p = N/2$, $K_s = 2N$.

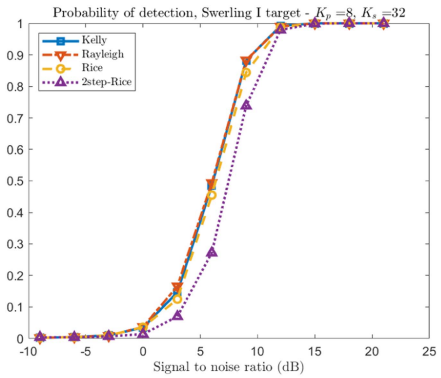

(a)

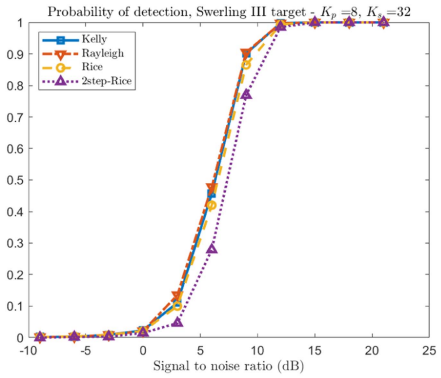

(b)

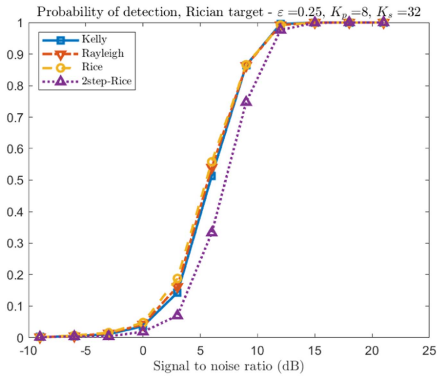

(c)

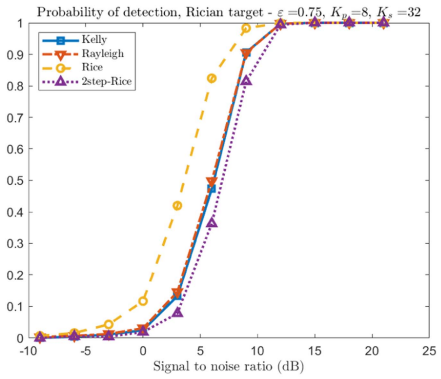

(d)

Fig. 4. Probability of detection versus SNR. $K_p = N/2$ and $K_s = 2N$. (a) Swerling I. (b) Swerling III. (c) Rician $\varepsilon = 0.25$. (d) Rician $\varepsilon = 0.75$.

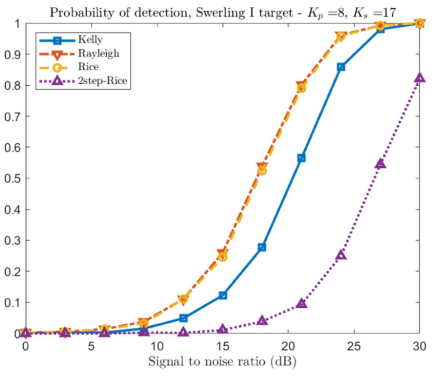

(a)

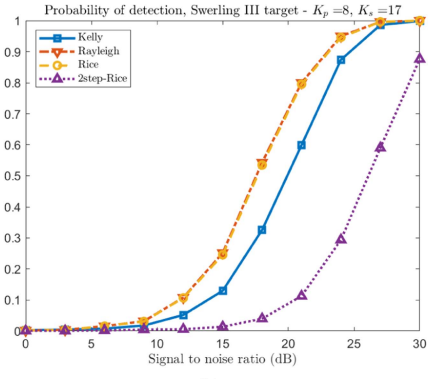

(b)

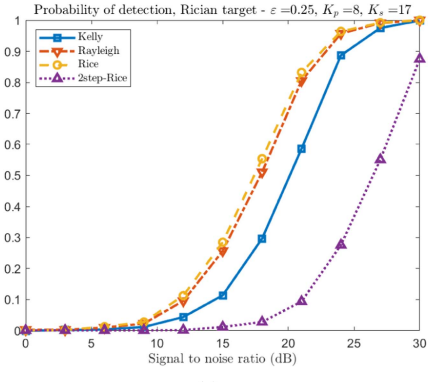

(c)

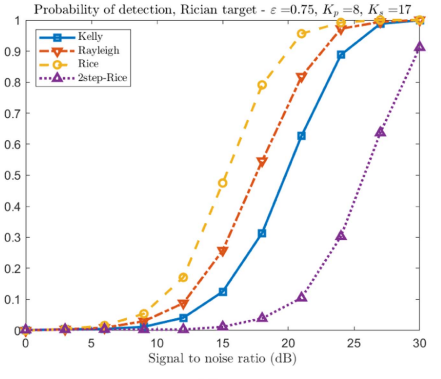

(d)

Fig. 5. Probability of detection versus SNR. $K_p = N/2$ and $K_s = N + 1$. (a) Swerling I. (b) Swerling III. (c) Rician $\varepsilon = 0.25$. (d) Rician $\varepsilon = 0.75$.

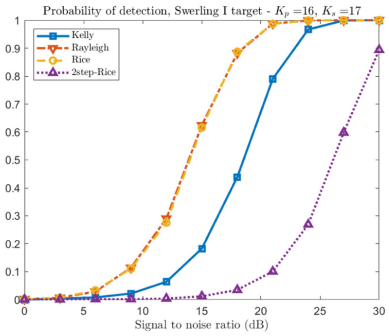

(a)

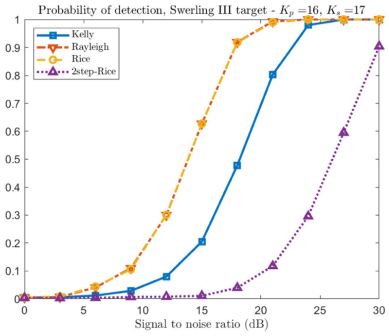

(b)

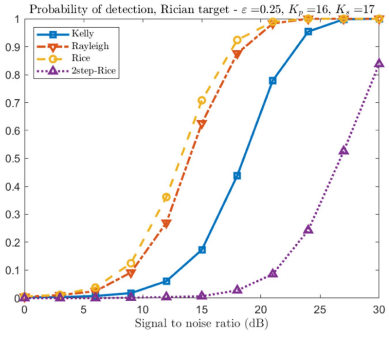

(c)

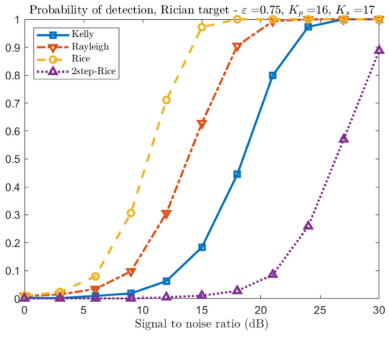

(d)

Fig. 6. Probability of detection versus SNR. $K_p = N$ and $K_s = N + 1$. (a) Swerling I. (b) Swerling III. (c) Rician $\varepsilon = 0.25$. (d) Rician $\varepsilon = 0.75$.

a Swerling III target, which makes sense. Overall, the target power is rather well estimated.

B. Detection

We now evaluate the detection performance of the new detectors and compare their probability of detection with that of Kelly's GLRT and the GLRT for Swerling I targets [5]. The probability of false alarm is set to $P_{\text{fa}} = 10^{-3}$, and the probability of detection is obtained from 1000 Monte Carlo trials. First, we consider a scenario with a rather large number of training samples, namely, $K_s = 2N$, and we compare the four detectors in Fig. 4. As can be observed, there is almost no difference between Kelly's GLRT, the Swerling I GLRT, and the Rician GLRT for Swerling I targets, Swerling III targets, and Rician targets with $\varepsilon = 0.25$. However, when $\varepsilon = 0.75$, the new Rician GLRT outperforms the two other detectors. Note that in no case, even Swerling I, is the new detector worse than the other ones. We also notice that, despite $K_s = 2N$, the two-step Rician GLRT performs worse than the three one-step GLRTs on all types of targets. In particular, its probability of detection is rather far from that of the Rician one-step GLRT for Rician targets.

Next, we consider a more challenging scenario with a small number of training samples, i.e., $K_s = N + 1$, and we set $K_p = N/2$ in Fig. 5 and $K_p = N$ in Fig. 6. First, it can be observed that, with this smaller value of K_s, Kelly's GLRT and, still worse, the two-step Rician GLRT suffer from a significant loss of detection capability. The new Rician GLRT is seen to perform as well as the Swerling I GLRT for Swerling I and III targets and has a higher P_d for Rician targets, either with $\varepsilon = 0.25$ or $\varepsilon = 0.75$. The difference is seen to increase when K_p increases. For instance when $\varepsilon = 0.75$, the improvement compared to the Swerling I GLRT is about 2 dB for $K_p = N/2$ and 3.5 dB for $K_p = N$.

IV. CONCLUSION

In this article, we addressed the adaptive detection of Rician targets in unknown Gaussian noise. The MLEs of the unknown parameters under each hypothesis were derived, from which the GLRT followed and was shown to have a CFAR. The performance of the MLE and the GLRT was evaluated for different types of targets, namely, Swerling I, Swerling III, and Rician. As for estimation, the MLEs of the Rician parameters $(|\bar{a}|^2, \sigma_a^2)$ were shown to be pretty accurate, at least with a sufficient number of training samples. For Swerling targets where the square amplitude $|a|^2$ follows a chi-square distribution, the MLE is able to balance the respective contributions of $|\bar{a}|^2$ and σ_a^2, the former being small while the latter is about the target power. Hence, these estimates could serve as an indicator of the type of targets. As for detection, we showed that the new detector is as good as Kelly's GLRT for all types of targets when $K_s = 2N$ and outperforms Kelly's GLRT for small K_s. In addition, it incurs no loss compared to the Swerling I GLRT for Swerling targets. Finally, it provides a significant improvement over both detectors for Rician targets even with a small proportion of the dominant scatterer. Therefore, it offers the most interesting solution for a large variety of targets.

OLIVIER BESSON
ISAE-SUPAERO, Université de Toulouse, Toulouse, France

REFERENCES

[1] E. J. Kelly, "An adaptive detection algorithm," *IEEE Trans. Aerosp. Electron. Syst.*, vol. AES-22, no. 2, pp. 115–127, Mar. 1986.

[2] E. J. Kelly and K. M. Forsythe, "Adaptive detection and parameter estimation for multidimensional signal models," Massachusetts Inst. Technol. Lincoln Lab., Lexington, MA, USA, Tech. Rep. 848, 1989.

[3] P. Swerling, "Probability of detection for fluctuating targets," *IRE Trans. Inf. Theory*, vol. 6, no. 2, pp. 269–308, Apr. 1960.

[4] P. Swerling, "Radar probability of detection for some additional fluctuating target cases," *IEEE Trans. Aerosp. Electron. Syst.*, vol. 33, no. 2, pp. 698–709, Apr. 1997.

[5] O. Besson, A. Coluccia, E. Chaumette, G. Ricci, and F. Vincent, "Generalized likelihood ratio test for detection of Gaussian rank-one signals in Gaussian noise with unknown statistics," *IEEE Trans. Signal Process.*, vol. 65, no. 4, pp. 1082–1092, Feb. 2017.

[6] E. Chaumette, F. Vincent, and G. Ginolhac, "Detection of Swerling III-IV rank-one signals in Gaussian noise with unknown statistics," in *Proc. 52nd Asilomar Conf. Signals, Syst., Comput.*, 2018, pp. 2072–2076.

[7] M. I. Skolnik, *Introduction to Radar Systems*, 2nd ed. New York, NY, USA: McGraw-Hill, 1981.

[8] X. Song, W. D. Blair, P. Willett, and S. Zhou, "Dominant-plus-Rayleigh models for RCS: Swerling III/IV versus Rician," *IEEE Trans. Aerosp. Electron. Syst.*, vol. 49, no. 3, pp. 2058–2064, Jul. 2013.

[9] C. D. Papanicolopoulos, W. D. Blair, D. L. Sherman, and M. Brandt-Pearce, "Use of a Rician distribution for modeling aspect-dependent RCS amplitude and scintillation," in *Proc. IEEE Radar Conf.*, 2007, pp. 218–223.

[10] A. Dogandzic and J. Jinghua, "Estimating statistical properties of MIMO fading channels," *IEEE Trans. Signal Process.*, vol. 53, no. 8, pp. 3065–3080, Aug. 2005.

[11] P. F. Sammartino, C. J. Baker, and H. D. Griffiths, "Target model effects on MIMO radar performance," in *Proc. IEEE Int. Conf. Acoust., Speech, Signal Process.*, 2006, pp. 1129–1132.

[12] B. Tang, J. Tang, and Y. Zhang, "Design of multiple-input–multiple-output radar waveforms for Rician target detection," *IET Radar, Sonar Navigation*, vol. 10, no. 9, pp. 1583–1593, 2016.

[13] O. Ozdogan, E. Bjornson, and E. G. Larsson, "Massive MIMO with spatially correlated Rician fading channels," *IEEE Trans. Commun.*, vol. 67, no. 5, pp. 3234–3250, May 2019.

[14] X. Wang, B. Tang, and M. Zhang, "Optimisation of practically constrained waveforms for Rician target detection with multiple-input-multiple-output radar," *IET Radar, Sonar Navigation*, vol. 16, no. 7, pp. 1116–1130, 2022.

[15] F. C. Robey, D. R. Fuhrmann, E. J. Kelly, and R. Nitzberg, "A CFAR adaptive matched filter detector," *IEEE Trans. Aerosp. Electron. Syst.*, vol. 28, no. 1, pp. 208–216, Jan. 1992.